J. Fluid Mech. (1969), *vol.* 38, *part* 4, *pp.* 743–763
Printed in Great Britain

Measurements of spectral energy transfer in grid turbulence

By C. W. VAN ATTA† AND W. Y. CHEN

Department of the Aerospace and Mechanical Engineering Sciences,
University of California, San Diego

(Received 7 February 1969)

Direct measurements of the energy transfer spectrum in locally isotropic grid turbulence have been used to determine the extent of validity for grid turbulence of the dynamical equation for the three-dimensional energy spectrum in isotropic turbulence. The extent of applicability of the isotropic energy balance is consistent with the usual local isotropy criterion based on energy spectra alone.

The present results are in general agreement with some previous measurements by Uberoi, who determined the transfer spectrum assuming the strict validity of the isotropic dynamical equation. The measured energy transfer spectra are quantitatively similar to those calculated by Kraichnan using the direct-interaction approximation.

1. Introduction

The complex, inherently non-linear process of spectral transfer of turbulent kinetic energy between continuously distributed scales of motion in a turbulent flow has been the subject of many analytical studies, but comparatively few experimental efforts have been directed at this central fluid-mechanical problem. The dynamical equation for the three-dimensional energy spectrum $E(k,t)$ in homogeneous, isotropic turbulence is

$$\frac{\partial E(k,t)}{\partial t} = T(k,t) - 2\nu k^2 E(k,t), \tag{1}$$

where $$\tfrac{1}{2}(\langle u^2\rangle + \langle v^2\rangle + \langle w^2\rangle) = \int_0^\infty E(k,t)\,dk,$$

and $T(k)$, the energy transfer spectrum, is a functional of the Fourier transform of the triple velocity correlation between a single velocity component taken at one point and two velocity components taken at another point in the turbulent field.

Equation (1) states that the rate of change of the energy spectrum at any given wave-number k is equal to the net rate of transfer of energy to wave-number k from all other wave-numbers minus the rate of viscous dissipation at wave-number k. As a result of the averaging process used to derive (1), the initial value problem for $E(k,t)$ is indeterminate, for we have two unknowns, E and T, related through a single equation. To solve for $E(k,t)$ in terms of $E(k,0)$, one may

† Also: Scripps Institution of Oceanography.

either postulate a relation between the rate of transfer T and the spectrum E, or carry out a numerical integration of the Fourier-transformed Navier–Stokes equation from which (1) is derived. Calculations of the latter type, which are clearly preferable to hypotheses lacking sound physical basis, have been carried out for decaying isotropic turbulence by Kraichnan (1964) using the direct-interaction approximation to evaluate the inertial interactions associated with $T(k, t)$.

Various investigators have proposed hypotheses relating T and E. As pointed out by Uberoi (1963), the validity of the various postulates may be checked by comparing the measured spectrum with the predicted spectrum, but a direct measurement of the energy transfer is a more direct check and brings out the essential features of the problem. For grid-generated turbulence, Uberoi has compared Heisenberg's postulate for $T(E)$ with experimentally determined $T(k, t)$ obtained from the sum of the measured $\partial E(k, t)/\partial t$ and $2\nu k^2 E(k, t)$, assuming the validity of (1).

In the present study the extent of the validity of (1) for grid-generated turbulence is determined by directly measuring all the terms in the equation. The measured $T(k, t)$ spectra are compared with those obtained indirectly by Uberoi, with direct-interaction calculations by Kraichnan, and with various hypotheses relating $T(k)$ and $E(k)$.

2. Experimental arrangement

The experiments were carried out in the 76 cm square test section of the low-turbulence wind-tunnel in the Department of the Aerospace and Mechanical Engineering Sciences. Biplane grids of round, polished dural rods were located 2·4 m from the end of the contraction section. Two different grids were used, having mesh spacings M of 2·54 and 5·08 cm with rods of 0·477 and 0·953 cm diameter, respectively. The mean velocity U was 15·7 m/s for the 2·54 cm grid measurements and 7·7 m/s for the 5·08 cm grid measurements, with corresponding Reynolds numbers based on mesh spacing of 25,600 and 25,300, respectively. These conditions were nearly the same as those used for measurements of higher-order time correlations of the longitudinal fluctuating component of velocity reported by Van Atta & Chen (1968). The high-speed, small-grid experimental conditions were nearly identical with those of Uberoi with respect to mesh spacing and mean velocity, but the grid rod diameter was different, as Uberoi used a biplane grid of 0·635 cm diameter wooden dowels. In the present experiments we have measured $T(k)$ only at $x/M = 48$, where x is the distance downstream of the grid, whereas Uberoi made (indirect) measurements of $T(k)$ at $x/M = 48$, 72 and 110.

An X-wire arrangement consisting of two mutually perpendicular tungsten hot wires, each 0·75 mm long and 5 μm in diameter, was used to measure u and v, the longitudinal and transverse components of the fluctuating velocity on the tunnel centreline. DISA 55 A 01 amplifiers were used to operate the hot wires at constant resistance, with an overheat ratio of 0·5. The hot-wire outputs were linearized using DISA 55 D 10 linearizers. The 11·5 cm long, 0·24 cm diameter hot-wire probe was held on the tunnel centreline by a vertical 1·27 cm diameter

aluminium rod extending through a slot in the top of the tunnel. The rod was supported by a calibration turntable mounted on a heavy aluminium plate. The plate was bolted to heavy chassis slides, which allowed the longitudinal position of the probe to be varied continuously with a minimal amount of friction and disturbance to the set-up. The turntable was equipped with a large circular protractor for measuring the yaw angle during probe calibration.

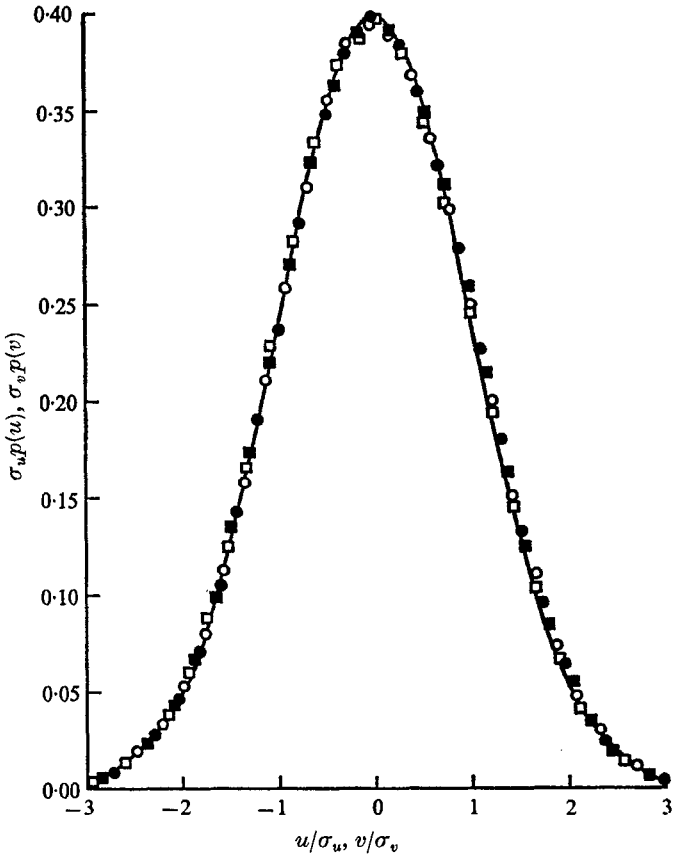

FIGURE 1. One-dimensional probability distributions for velocity fluctuations. U = 15·7 m/s: ●, u; ■, v. U = 7·7 m/s: ○, u; □, v. Solid line is Gaussian distribution.

The hot-wire calibrations were performed in laminar flow, with the grid removed from the tunnel. The probe was calibrated in yaw for several values of the free-stream velocity U and over a wide range of velocities for zero yaw angle. For the range of fluctuating velocities encountered in the turbulent flow, the sum and difference of the two linearized signals were found to be very closely linearly related to u and v, respectively. The resulting calibration constants were used to compute the velocity fluctuations from the sampled digital data and for a few analogue measurements made as a check on the digitally measured turbulence intensities. The results of the analogue measurements of u and v have been reported previously by Van Atta & Chen (1968, figure 1). The measurements showed that the decay of the normalized velocity fluctuations in the range $38 \leqslant x/M \leqslant 55$

was practically identical for both experimental conditions. The measured longitudinal turbulence levels at $x/M = 48$ were $\langle u^2\rangle^{\frac{1}{2}}/U = 1{\cdot}61 \times 10^{-2}$ for both high- and low-speed runs, and the ratio $(\langle u^2\rangle/\langle v^2\rangle)^{\frac{1}{2}}$, a measure of the over-all anisotropy of the turbulence, was 1·13 and 1·12 for the high- and low-speed runs, respectively.

The linearized hot-wire signals were FM tape recorded at a tape speed of 152·4 cm/s using a Sanborn 3917 A recorder. The analogue tape was later played back and sampled with an analogue-to-digital converter at a rate somewhat faster than twice the highest frequency for which the turbulent spectrum was unmistakably distinguishable from electronic noise. The sampling rates for the high- and low-speed data were 16,000 and 5600/s respectively.

The digital data were processed using a CDC 3600 computer. As an initial step, the running mean values of $\langle u^2\rangle$, $\langle v^2\rangle$, $\langle u^3\rangle$ and $\langle v^3\rangle$ were computed to determine the amount of data necessary to provide stationary values of these quantities. Sampling time intervals of 25·6 and 54·9 s were found to be adequate for high- and low-speed data, respectively. All subsequently computed spectra were based on one data record of this length, and all third-order correlations were based on averages of four such records. All spectra and correlation functions were computed from the two time series of sampled data for u and v using the discrete fast-Fourier-transform method. The data were transformed in records containing 2048 digital velocities and were processed in the manner previously described by Van Atta & Chen (1968, 1969).

3. Distribution of velocity fluctuations

The one-dimensional probability densities

$$p(u/\sigma_u) \quad \text{and} \quad p(v/\sigma_v),$$

where

$$\sigma_u = \langle u^2\rangle^{\frac{1}{2}} \quad \text{and} \quad \sigma_v = \langle v^2\rangle^{\frac{1}{2}},$$

were found to be closely Gaussian, as shown in figure 1. The joint probability density for the two velocity components u and v measured instantaneously at the same point $p[u(t), v(t)]$ was found to be closely fitted by a bivariate Gaussian distribution with zero correlation, as illustrated in figure 2. These results indicate that simultaneous values of u and v measured at the same point in grid turbulence are statistically independent. As a further check of statistical independence, the probability density of the instantaneous product uv was calculated. With the assumption of statistical independence, the probability density of the product of two Gaussian variables u and v is

$$p(uv) = \frac{1}{\pi\sigma_u\sigma_v} K_0\left(\frac{|uv|}{\sigma_u\sigma_v}\right),$$

where K_0 is the modified Bessel function of the second kind. The good agreement between this expression and the measured density, shown in figure 3, further confirms the statistical independence of u and v. This is also consistent with the result reported by Van Atta & Chen (1969) that for these same data the correlation $R_{u,v}(\tau) = \langle u(t)\, v(t+\tau)\rangle/\langle u^2\rangle^{\frac{1}{2}}\langle v^2\rangle^{\frac{1}{2}}$ is essentially zero for all values of τ, as one would expect for unsheared laterally homogeneous grid tubulence.

4. Energy spectra

The three-dimensional energy spectrum $E(k, t)$ was determined from the one-dimensional energy spectra E_{11} and E_{22} of the u and v components, respectively. These were directly calculated from the discrete Fourier transforms of the time

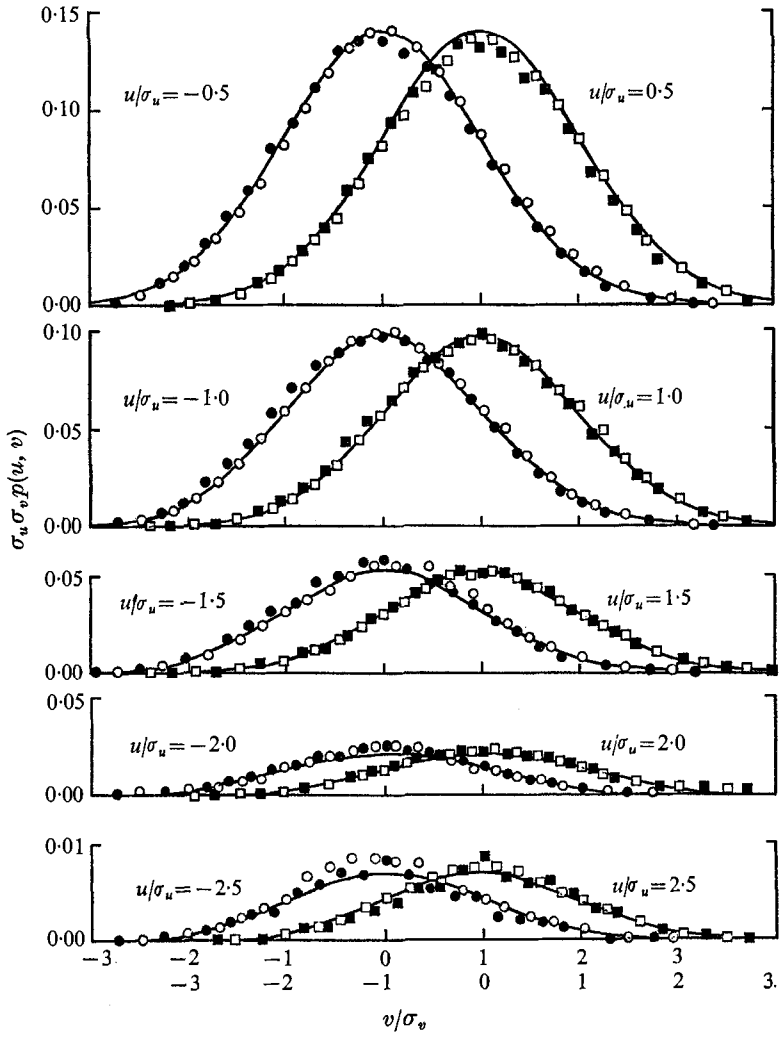

FIGURE 2. Joint probability distributions for u and v for selected values of u/σ_u. Solid symbols, U = 15·7 m/s; open symbols, U = 7·7 m/s. Solid curves are two-dimensional Gaussian distribution.

series for instantaneous values of u and v. The data were transformed in records containing 2048 digital velocities and were processed exactly as described previously by Van Atta & Chen (1968, 1969).

The measured $E_{11}(k_1)$ and $E_{22}(k_1)$ for $x/M = 48$ are shown in figure 4. The

extent of local isotropy was determined by comparing the measured $E_{22}(k_1)$ with the $E_{22}(k_1)$ calculated from the measured $E_{11}(k_1)$ using the isotropic relation

$$E_{22}(k_1) = \frac{1}{2}\left[E_{11}(k_1) - k_1 \frac{\partial E_{11}(k_1)}{\partial k_1}\right].$$

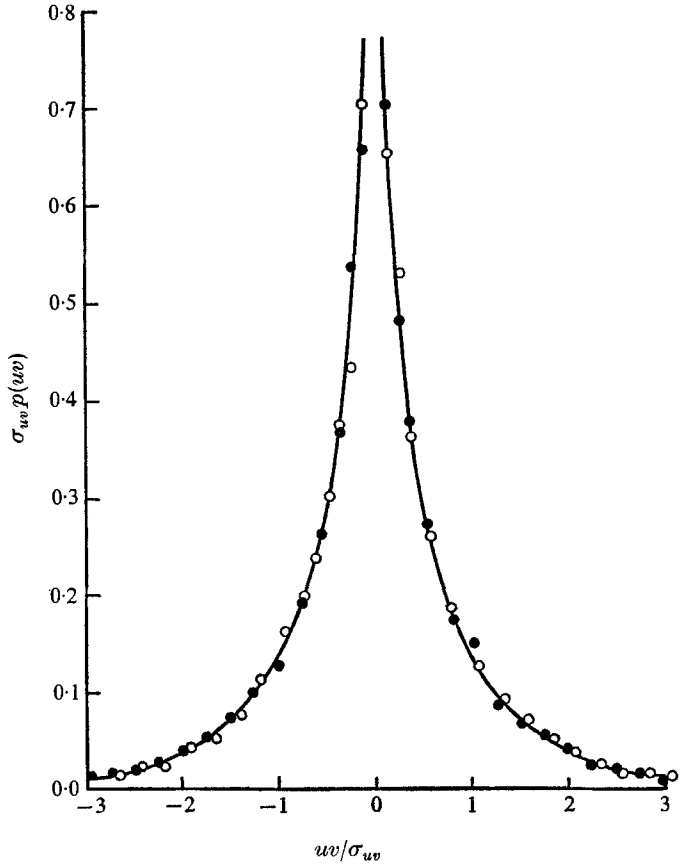

FIGURE 3. Probability distribution of instantaneous values of uv. ●, U = 15·7 m/s; ○, U = 7·7 m/s. Solid curve: $p(uv) = (1/\pi\sigma_u\sigma_v)\, K_0(|uv|/\sigma_u\sigma_v)$.

From the comparison in figure 4, it is found that the turbulence is closely locally isotropic for $k_1 \geqslant 1{\cdot}0\,\mathrm{cm}^{-1}$ and $k_1 \geqslant 0{\cdot}5\,\mathrm{cm}^{-1}$ for the high- and low-speed data, respectively, which in both cases corresponds to $k/k_K = 0{\cdot}24$. Here, $k_1 = 2\pi f/U$, where f is frequency (H_z) and $k_K = (\epsilon/\nu^3)^{\frac{1}{4}}$ is the Kolmogoroff wave-number.

Assuming that by symmetry the spectrum $E_{33}(k_1)$ of the w component was equal to $E_{22}(k_1)$, the one-dimensional spectrum $E_{ii}(k_1)$ of the total energy was computed from the measured $E_{11}(k_1)$ and $E_{22}(k_1)$, where

$$\langle u^2\rangle + \langle v^2\rangle + \langle w^2\rangle = 2\int_0^\infty E_{ii}(k_1)\, dk_1$$

and

$$E_{ii}(k_1) = E_{11}(k_1) + 2E_{22}(k_1).$$

We note that our definition of $E_{ii}(k_1)$ differs from Uberoi's one-dimensional total energy spectrum $E_1(k_1)$ by a factor of two. Uberoi employed a single inclined hot wire to measure instantaneous values of $u+\sqrt{(2)}\,v$ and did not obtain u and v (and hence $E_{11}(k_1)$ and $E_{22}(k_1)$) separately as we have done. The present

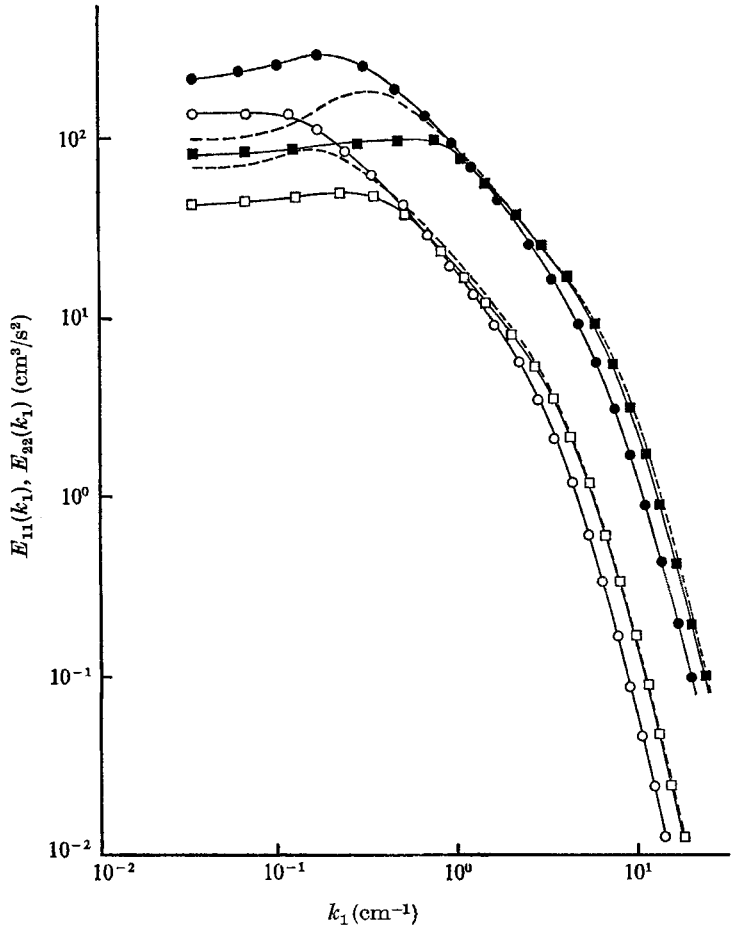

FIGURE 4. One-dimensional energy spectra for u and v. U = 15·7 m/s: ●, E_{11}; ■, E_{22} U = 7·7 m/s: ○, E_{11}; □, E_{22}. Dashed curves are values of E_{22} calculated from corresponding E_{11} using isotropic relation.

measured $E_{ii}(k_1)$ spectra and those of Uberoi, normalized using the Kolmogoroff length scale k_K^{-1} and velocity scale $v_K = (\epsilon\nu)^{\frac{1}{4}}$, are shown in figure 5. Here, as previously, the dissipation rate $\epsilon = -\frac{1}{2}\,d/dt(\langle u^2\rangle + 2\langle v^2\rangle)$ was computed from the slopes of plots of $U^2/(\langle u^2\rangle + 2\langle v^2\rangle)$ versus x/M. Values for ϵ and other parameters, useful in comparing the present data with that of Uberoi, are given in table 1. As expected, for high enough wave-numbers the spectra define a single universal curve. The differences at low wave-number reflect the differences in the energy-containing eddies, and this difference decreases as Uberoi's x/M increases. The present $E_{ii}(k)$ for U = 15·7 m/s is quite similar to, but smaller than, that obtained for x/M = 48 by Uberoi, since the turbulent intensities for a given x/M are

	Present measurements		Uberoi (1963)		
U (m/s)	15·7	7·7	15·7	15·7	15·7
M (cm)	2·54	5·08	2·54	2·54	2·54
d (cm)	0·477	0·953	0·635	0·635	0·635
R_M	25,600	25,300	26,400	26,400	26,400
x/M	48	48	48	72	110
$\langle u^2\rangle^{\frac{1}{2}}/U$	0·0161	0·0161	0·0214	0·0162	0·0124
R_λ	49·4	34·6	75	67	70
ϵ (cm^2/s^3)	$1{\cdot}24\times10^4$	$7{\cdot}87\times10^2$	$1{\cdot}95\times10^4$	$8{\cdot}44\times10^3$	$3{\cdot}42\times10^3$

TABLE 1

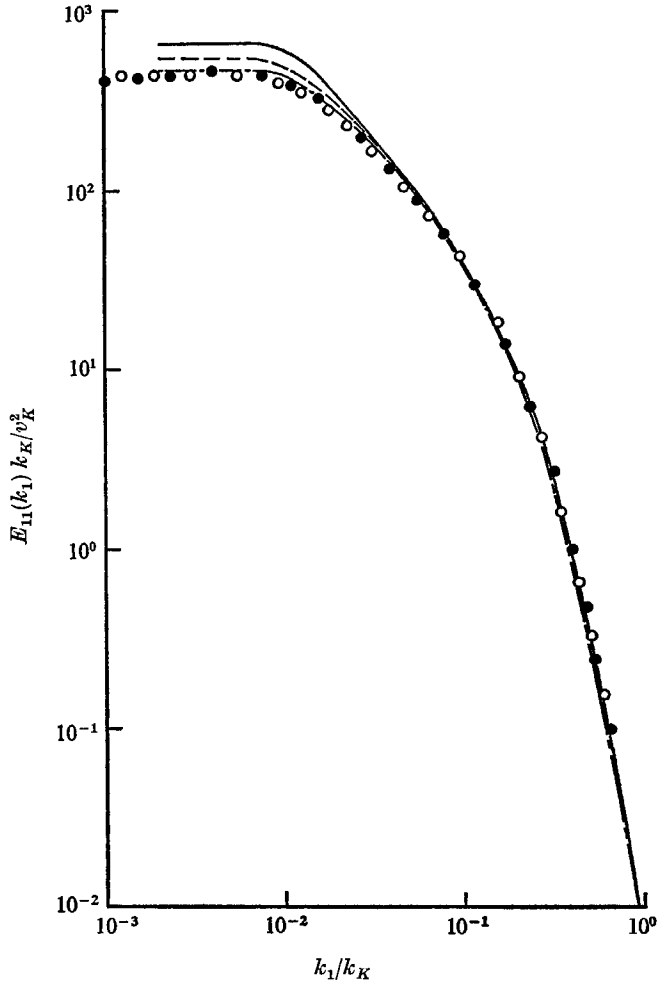

FIGURE 5. Normalized one-dimensional spectra of total energy. ●, U = 15·7 m/s: ○, U = 7·7 m/s. Uberoi: —, x/M = 48; – – –, x/M = 72; – · –, x/M = 110.

smaller in the present experiment. This difference reflects the fact that Uberoi used a 1 in. mesh grid with 0·635 cm diameter wooden dowels, whereas our 1 in. grid was constructed of 0·477 cm diameter polished aluminium rods.

The three-dimensional energy spectrum was calculated using the isotropic relation

$$E(k) = -k\frac{dE_{ii}(k)}{dk}, \tag{2}$$

where $$k = (k_1^2 + k_2^2 + k_3^2)^{\frac{1}{2}}.$$

If we had measured only the spectrum of u or v, it would have been necessary to differentiate the measured spectrum twice in order to obtain $E(k)$. This would produce unacceptably large uncertainties in $E(k)$. We used Uberoi's logarithmic differentiation method to determine $E(k)$ from $E_{ii}(k_1)$, since this procedure is much more accurate than direct differentiation.

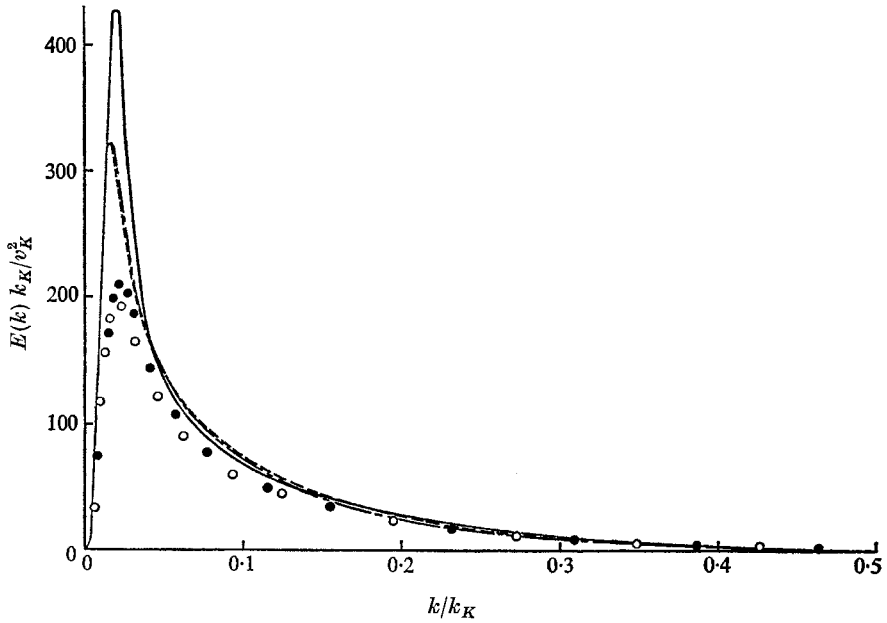

FIGURE 6. Normalized three-dimensional energy spectra. ●, U = 15·7 m/s: ○, U = 7·7 m/s. Uberoi: ——, x/M = 48; - - -, x/M = 72; – – –, x/M = 110.

The computed $E(k)$ spectra and the dissipation spectra $2\nu k^2 E(k)$ normalized with the Kolmogoroff length scales and velocity scale are presented in figures 6 and 7 and compared with the measurements of Uberoi. As expected, the energy spectra exhibit maxima at $k \sim 1/M$. The values of E at high wave-numbers are too small to present in figure 6. There is fair agreement with Uberoi's $E(k)$ spectrum for $x/M = 48$, except for wave-numbers near $k \sim 1/M$. Agreement should not be expected in this (the energy-containing) range because of the difference in turbulence intensities in the two experiments and the fact that Kolmogoroff scaling is not expected to apply in this range. For U = 15·7 m/s, the values of k/k_K corresponding to the maximum values of the energy and dissipation spectra are in close agreement with those obtained by Uberoi for

$x/M = 48$. The present normalized dissipation spectra, which emphasize the higher wave-numbers, are in fairly good agreement with Uberoi's dissipation spectrum for $x/M = 48$ over the entire wave-number range.

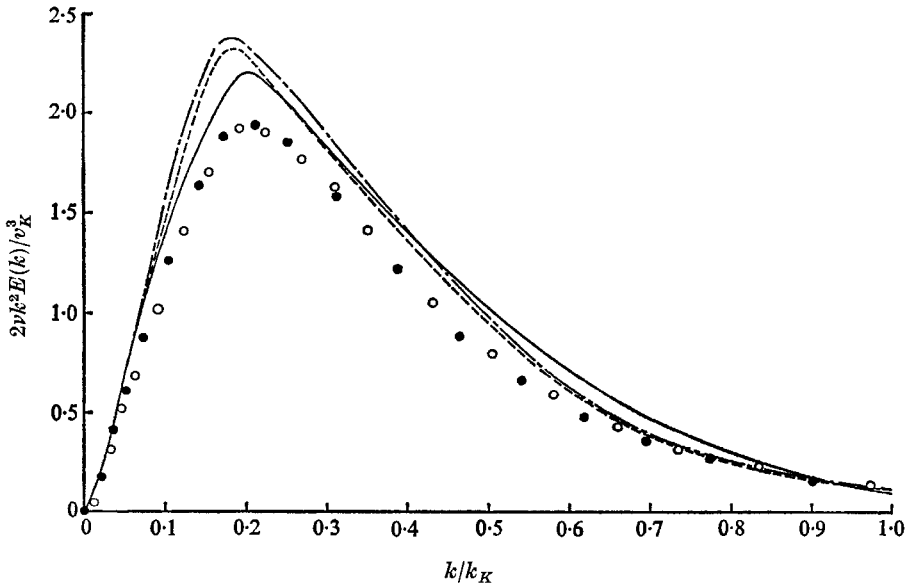

FIGURE 7. Normalized three-dimensional dissipation spectra. ●, $U = 15{\cdot}7$ m/s; ○, $U = 7{\cdot}7$ m/s. Uberoi: ——, $x/M = 48$; - - -, $x/M = 72$; – · –, $x/M = 110$.

The rate of change of the energy spectrum $\partial E/\partial t$ was determined from the decay of $E_{ii}(k_1)$ using the relation

$$\frac{\partial E}{\partial t} = -k\frac{\partial}{\partial k}\left(\frac{\partial E_{ii}}{\partial t}\right) = -kU\frac{\partial}{\partial k}\left(\frac{\partial E_{ii}}{\partial x}\right).$$

The one-dimensional energy spectrum $E_{ii}(k_1)$ was measured at seven locations in the range $38 \leqslant x/M \leqslant 55$. The derivative

$$\frac{d\log E_{ii}}{dx} = \beta(k) \quad \text{at} \quad x/M = 48$$

was then measured as a function of k. The data for $\partial E_{ii}/\partial t = UE_{ii}\beta$ are shown in figure 8. The slopes

$$\gamma(k) = \frac{\partial \log U\beta E_{ii}}{\partial \log k}$$

were also measured for $x/M = 48$, and $\partial E/\partial t$ was computed from the relation

$$\partial E/\partial t = -U\gamma(k)\,\beta(k)\,E_{ii}(k).$$

This is essentially the same procedure as followed by Uberoi, with the exception that Uberoi obtained a continuous measurement of $E_{ii}(k_1)$ as a function of x for fixed values of k_1 from an analogue plot† of his wave analyzer output as the probe was slowly traversed in the stream direction. The present data for $\partial E(k,t)/\partial t$, normalized with the Kolmogoroff velocity scale v_K, are compared

† M. S. Uberoi (private communication).

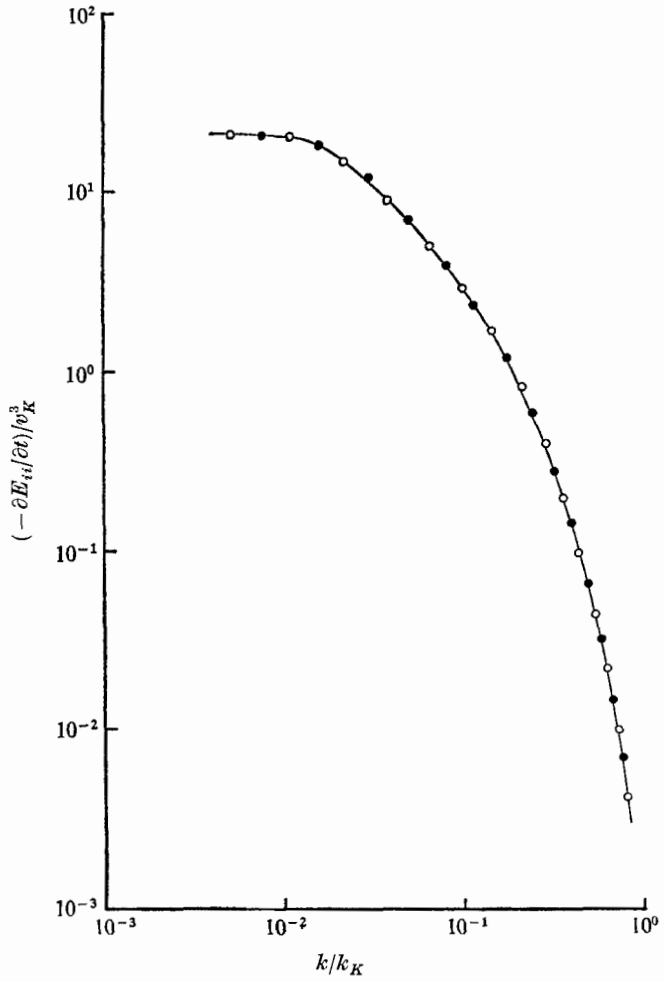

FIGURE 8. Rate of change of one-dimensional total energy spectrum. ●, $U = 15{\cdot}7$ m/s; ○, $U = 7{\cdot}7$ m/s.

with those of Uberoi in figure 9. The present normalized data and those of Uberoi for $x/M = 48$ are in fairly good agreement for large wave-numbers (k/k_K greater than about 0·2), as would be expected for the locally isotropic range of wave-numbers. For isotropic turbulence, the integrated energy transfer is zero and

$$\int_0^\infty \frac{\partial E}{\partial t}\,dk = -2\nu\int_0^\infty k^2 E\,dk,$$

or

$$U\int_0^\infty \gamma\beta E_{ii}\,dk = 2\nu\int_0^\infty k^2 E\,dk. \tag{3}$$

For the present data, the measured values of the right-hand side of (3) are about 26 % smaller than the left-hand side. For $x/M = 48$, Uberoi found a similar discrepancy of 13 %. In both cases, the discrepancy is most certainly due to the inapplicability for low wave-numbers of the isotropic relations used to derive

$E(k,t)$ and $\partial E(k,t)/\partial t$ from the one-dimensional spectra. In spite of this difficulty, Uberoi then enforced the equality of (3) by multiplying the measured β by a constant factor (0·87 for $x/M = 48$), and then calculated $T(k,t)$ from the relation

$$T(k,t) = \frac{\partial E(k,t)}{\partial t} + 2\nu k^2 E(k,t).$$

We shall demonstrate below that this arbitrary procedure, which heavily weights contributions from non-isotropic low wave-numbers, can lead to misleading results in the over-all energy balance for higher wave-numbers in the locally isotropic range.

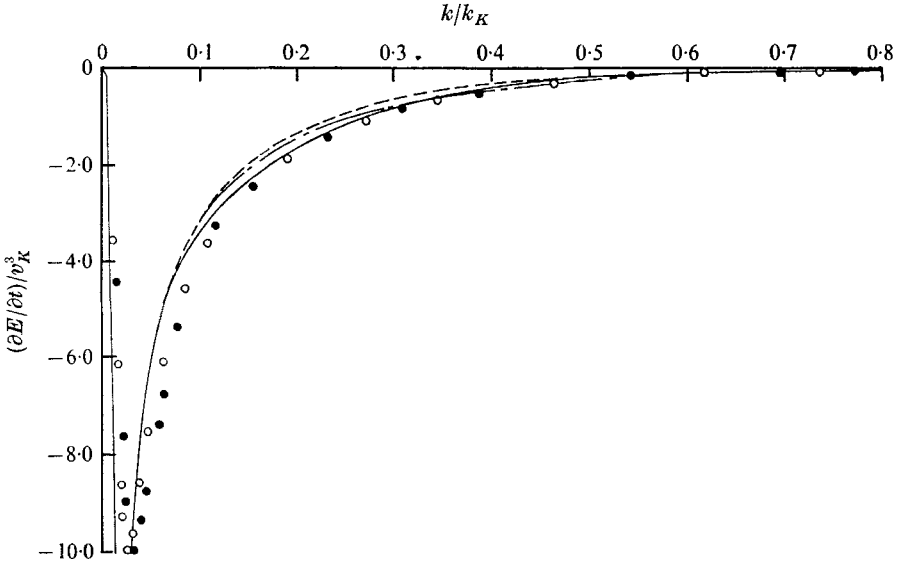

FIGURE 9. Rate of change of three-dimensional energy spectrum. ●, U = 15·7 m/s; ○, U = 7·7 m/s. Uberoi: ——, $x/M = 48$; - - -, $x/M = 72$; – · –, $x/M = 110$.

5. Energy transfer spectra

The three-dimensional energy transfer spectrum $T(k,t)$ was computed from the measured triple correlation functions. Following Batchelor's (1953) notation wherever possible, we define the two-point third-order velocity correlation tensor $S_{ij}(\bar{r})$ and its corresponding spectral tensor $\Gamma_{ij}(\bar{k})$ by the relations

$$S_{ij}(\bar{r}) = \langle u_i(\bar{x})\, u_i(\bar{x})\, u_j(\bar{x}+\bar{r})\rangle = \int_{-\infty}^{\infty}\int_{-\infty}^{\infty}\int_{-\infty}^{\infty} \Gamma_{ij}(\bar{k})\, e^{i\bar{k}\cdot\bar{r}}\, d\bar{k}.$$

Taking $\bar{r}$ in the x-direction (direction of U), we have for the sum of the three correlations $S_{111}(r_1)$, $S_{212}(r_1)$ and $S_{313}(r_1)$

$$\begin{aligned} S_{iii}(r_{1,0,0}) &= \int_{-\infty}^{\infty}\int_{-\infty}^{\infty}\int_{-\infty}^{\infty} \Gamma_{iii}(\bar{k})\, e^{ik_1 r_1}\, dk_1\, dk_2\, dk_3 \\ &= \int_{-\infty}^{\infty} e^{ik_1 r_1}\left[\int_{-\infty}^{\infty}\int_{-\infty}^{\infty} \Gamma_{iii}(\bar{k})\, dk_2\, dk_3\right] dk_1. \end{aligned} \tag{4}$$

Defining a function $L(k)$ such that

$$-iL(k_1)/k_1 = \int_{-\infty}^{\infty}\int_{-\infty}^{\infty} \Gamma_{i1i}(\bar{k})\, dk_2\, dk_3, \tag{5}$$

and taking the one-dimensional Fourier transform of (4), we find that

$$L(k_1) = \frac{ik_1}{2\pi}\int_{-\infty}^{\infty} S_{i1i}(r_{1,0,0})\, e^{-ik_1 r_1}\, dr_1. \tag{6}$$

$L(k_1)$ plays the role of a measurable one-dimensional energy transfer function from which $T(k,t)$ may be derived. From Batchelor (1953) we have, for isotropic turbulence,

$$\Gamma_{i1i}(\bar{k}) = -\frac{ik_1 T(k)}{4\pi k^4}.$$

Substituting for $\Gamma_{i1i}(\bar{k})$ in (5) we have

$$L(k_1)/k_1^2 = \int_{-\infty}^{\infty}\int_{-\infty}^{\infty} \frac{T(k)}{4\pi k^4}\, dk_2\, dk_3.$$

Transforming to polar co-ordinates $\zeta = (k_2^2 + k_3^2)^{\frac{1}{2}}$ and θ, and integrating over θ, we obtain

$$L(k_1)/k_1^2 = \int_{-\infty}^{\infty} \frac{T(k)}{2k^4}\,\zeta\, d\zeta = \int_{k_1}^{\infty} \frac{T(k)}{2k^3}\, dk$$

since $k^2 = \zeta^2 + k_1^2$. Differentiating with respect to k_1, we find

$$T(k) = 4L(k) - 2k\frac{dL(k)}{dk}. \tag{7}$$

Using this relation, we can calculate $T(k,t)$ from the measurable one-dimensional transfer spectrum $L(k)$ with only a single differentiation. It is possible to derive similar relations for $T(k,t)$ depending on one-dimensional spectra which are the one-dimensional Fourier transforms of only a single triple correlation, but such expressions for $T(k,t)$ invariably involve second derivatives of the transforms, and hence would lead to unacceptable uncertainties when applied to experimental data. The situation is somewhat analogous to that encountered when determining $E(k,t)$ from one-dimensional energy spectra. Integral relations for T in terms of correlation functions are also available, but our experience has been that the particular combinations of trigonometric and algebraic functions encountered in these expressions preclude sufficiently accurate numerical integration, especially for large values of k. We therefore have been led to work with the combination $S_{i1i}(r_1)$, hoping that such a procedure may also help to minimize the effects of anistropy at the smaller wave-numbers.

To ensure that $L(k)$ is a real function requires that $S_{111}(r_1)$, $S_{212}(r_1)$ and $S_{313}(r_1)$ be odd functions of r_1. As shown in some of our previously reported measurements (Van Atta & Chen 1969), we find that these correlations, measured at a single point, are in fact nearly odd functions of the time delay τ, and, assuming that $r_1 = U\tau$, nearly odd functions of r_1. In order to apply (6) in the present study, we have replaced each approximately antisymmetrical measured $S_{ilj}(r_1)$ by an

exactly antisymmetrical function formed from one-half of the difference of the measured correlations for positive and negative r_1. That is, we replaced

$$S_{111}(r_1) \quad \text{by} \quad S^*_{111}(r_1) = \tfrac{1}{2}[S_{111}(r_1) - S_{111}(-r_1)]$$

and

$$S_{212}(r_1) \quad \text{by} \quad S^*_{212}(r_1) = \tfrac{1}{2}[S_{212}(r_1) - S_{212}(-r_1)].$$

Noting that $\langle u^2(t)\, u(t-\tau)\rangle = \langle u(t)\, u^2(t+\tau)\rangle$, $S^*_{111}(r_1)$ is identical with the composite triple correlation measured by Frenkiel & Klebanoff (1967*a*, *b*) and by Van Atta & Chen (1968). Although these two investigations produced strikingly different individual triple correlations, the composite triple correlations are in good agreement. As reported previously (Van Atta & Chen 1969), the present

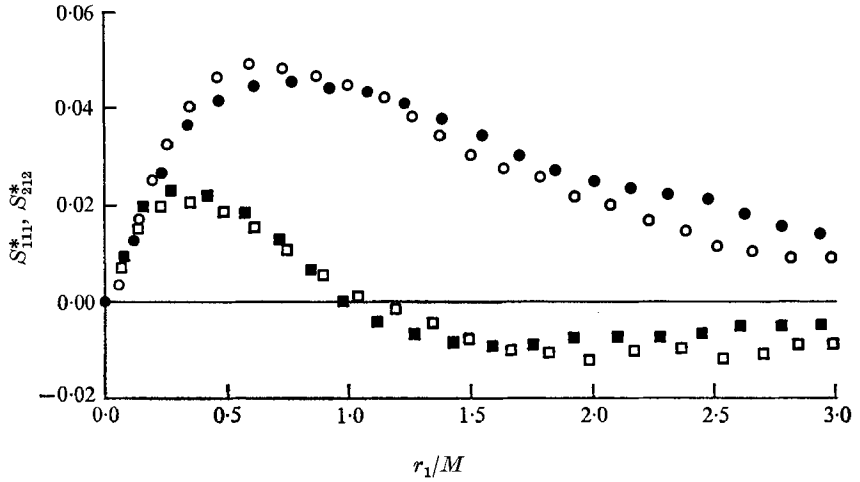

FIGURE 10. Normalized triple correlations. $U = 15{\cdot}7$ m/s: ●, S^*_{111}; ■, S^*_{212}. $U = 7{\cdot}7$ m/s: ○, S^*_{111}; □, S^*_{212}.

measured individual triple correlations for the longitudinal component ($S_{111}(r_1)$) are in good agreement with our previous measurements made with a single hot wire. The triple correlations $S^*_{111}(r_1)$ and $S^*_{212}(r_1)$, normalized with $\langle u^3\rangle$ and $\langle uv^2\rangle$ respectively, are shown in figure 10 for values of $U\tau/M$ up to 3·0. For larger values of $U\tau/M$, the correlations decay smoothly to zero. The discrete series of data points specifying each $S^*_{1i1}(r_1) = S^*_{111}(r_1) + 2S^*_{212}(r_1)$ as a function of τ was fast-Fourier-transformed to obtain $L(k_1)$ using (6). The functions obtained are shown in figure 11. We note that the scales in figure 11 for the high- and low-speed data differ by a factor of 10, reflecting the fact that a considerably larger amount of energy must be spectrally transferred in the higher-speed flow, for which the absolute turbulence intensity is larger and the dissipation higher. The three-dimensional energy transfer spectra $T(k)$, derived from the data of figure 11 using (7), have roughly the same relative amplitudes and shapes as the one-dimensional $L(k_1)$ spectra. The cross-over point from negative to positive net energy transfer occurs at wave-numbers of $k = 8{\cdot}5\ \text{cm}^{-1}$ and $k = 4{\cdot}3\ \text{cm}^{-1}$ for the high- and low-speed data, respectively, corresponding to length scales of about $0{\cdot}05M$. The negative maxima for low wave-numbers occurs at

$k = 1{\cdot}31\ \mathrm{cm}^{-1}$ and $k = 0{\cdot}66\ \mathrm{cm}^{-1}$ for the high- and low-speed data, respectively, corresponding to a length scale of $0{\cdot}3M$. The measured energy transfer spectra $T(k)$, normalized with the Kolmogoroff velocity $v_K = (\nu\epsilon)^{\frac{1}{4}}$, are plotted versus normalized wave-number in figure 12. The two normalized spectra collapse fairly well into a single curve, especially at the higher wave-numbers. For $k/k_K < 0{\cdot}2$, the net energy transfer at any given wave-number k is negative,

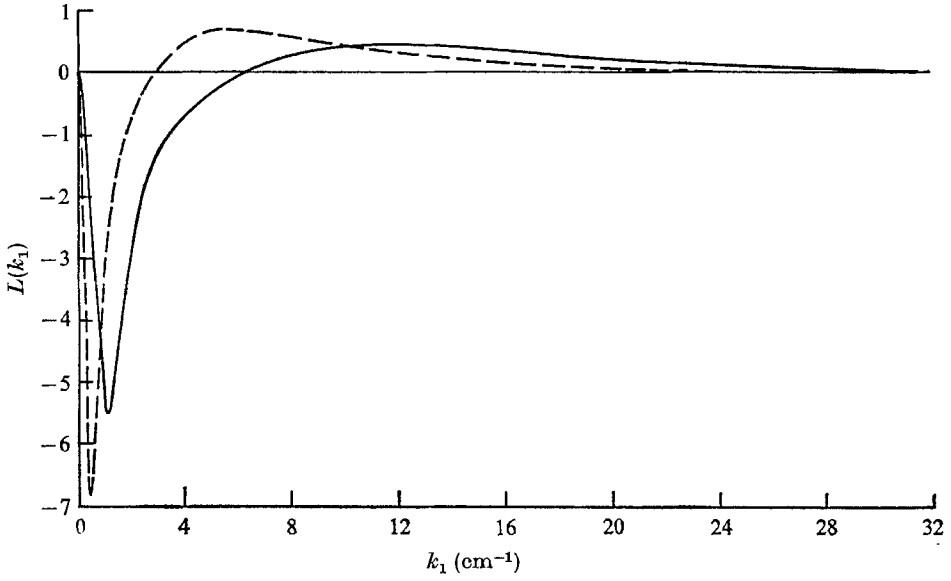

FIGURE 11. One-dimensional energy transfer functions. ——, $U = 15{\cdot}7$ m/s, $(\mathrm{cm/s})^3 \times 10^2$; - - -, $U = 7{\cdot}7$ m/s, $(\mathrm{cm/s})^3 \times 10^1$.

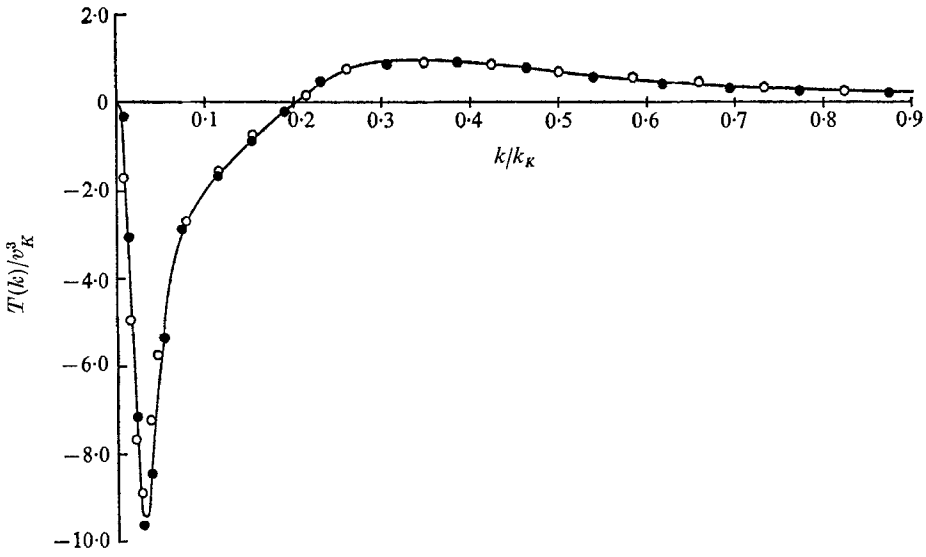

FIGURE 12. Measured three-dimensional energy transfer spectra. ●, $U = 15{\cdot}7$ m/s; ○, $U = 7{\cdot}7$ m/s.

and for $k/k_K > 0{\cdot}2$ the net transfer is positive. A broad maximum in the energy transferred to high wave-numbers occurs in the neighbourhood of $k/k_K = 0{\cdot}35$. The location of the negative maximum in the energy transferred from low wave-numbers which occurs at about $k/k_K = 0{\cdot}03$ is certainly of less significance, since the turbulence is not locally isotropic for such low wave-numbers, and use of the isotropic formulas used to derive $T(k)$ may produce misleading results. Comparing figures 7 and 12, we note that the maximum in the dissipation spectrum occurs almost precisely at the wave-number for which the net energy transfer is zero.

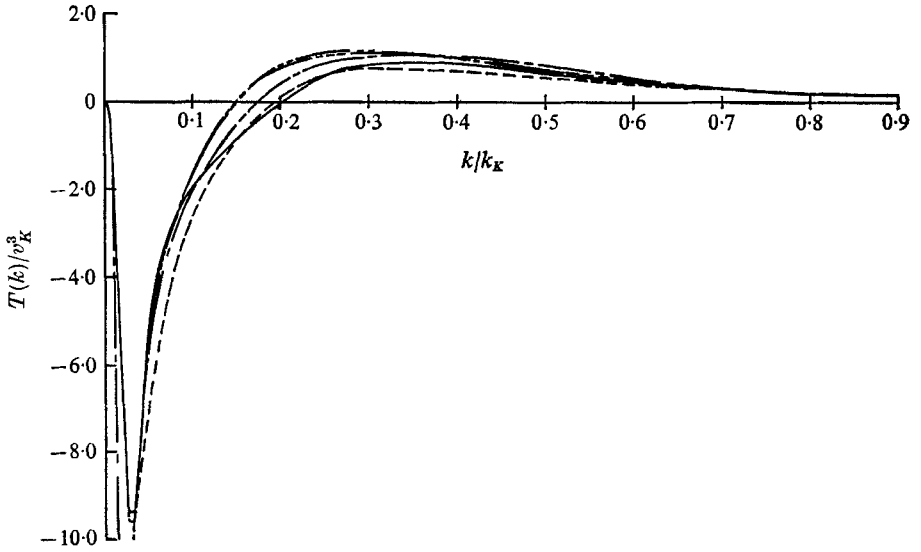

FIGURE 13. Comparison of directly measured transfer spectrum with isotropic dynamical equation and with results of Uberoi. ——, directly measured; - - -, computed from measured $(\partial E/\partial t) + 2\nu k^2 E$; Uberoi: – – –, $x/M = 48$; – · – ·, $x/M = 72$; – · · – ·, $x/M = 110$.

In figure 13 the extent of the validity of the isotropic relation of (1) for grid-generated turbulence is determined by comparing the directly measured energy transfer spectra with the measured values of $\{(\partial E/\partial t) + 2\nu k^2 E\}/v_K^3$, the sum being obtained from the data of figures 7 and 9. The directly measured $T(k)$ is in good agreement with the measured $\{(\partial E/\partial t) + 2\nu k^2 E\}$ for nearly the entire wave-number range in which the turbulence was previously found to be locally isotropic. The extent of agreement of the spectral energy balance with (1) is a higher-order criterion for local isotropy, as (1) contains third-order moments as compared with only the second-order moments (E_{11} and E_{22}) usually considered. However, because of the experimental uncertainties involved in obtaining the three-dimensional quantities in (1), the most we can conclude in the present case is that the extent of local isotropy is about the same as previously determined from E_{22} and E_{11} alone.

Also shown in figure 13 are Uberoi's data for the sum $\{(\partial E/\partial t) + 2\nu k^2 E\}/v_k^3$ calculated using his measured (non-adjusted, see § 4) values for β. All the normalized spectra, including those for Uberoi's three stations, are in good agree-

ment for $k/k_K \geqslant 0{\cdot}3$ and we conclude that the data represent the universal energy transfer spectrum in this range of wave-numbers. Noting that the turbulence is locally isotropic for $k/k_K \geqslant 0{\cdot}24$, we further tentatively conclude that our directly measured transfer spectrum in the range $k/k_K \geqslant 0{\cdot}2$ is a close approximation to the complete dissipative-range universal transfer spectrum that would be obtained for very large values of R_λ. A definitive experimental check of this conclusion would require that R_λ be large enough to produce an inertial subrange, in which $T(k,t)$ is zero, separating the energy-containing and dissipative ranges. If Uberoi's adjusted values for β are used, the agreement with our data is somewhat poorer and his data for the three values of x/M do not collapse as closely into a single curve. We conclude that Uberoi's enforcement of the equality of (3), and thereby the requirement that $\int_0^\infty T(k,t)\,dk$ be equal to zero, is inappropriate for grid turbulence, as the undue emphasis accorded by this procedure to the non-isotropic low wave-number range degrades the degree of similarity produced by Kolmogoroff scaling at larger wave-numbers where the turbulence is locally isotropic.

6. Comparison with direct-interaction calculations

The direct-interaction equations for the decay of isotropic turbulence have been integrated numerically by Kraichnan (1964), with initial spectra of several shapes and initial values of $R_\lambda \leqslant 40$. Kraichnan compared his results with measurements of one-dimensional longitudinal dissipation spectra in grid turbulence by Stewart & Townsend (1951). Considering his rather arbitrary choices of initial spectra, he found satisfactory quantitative agreement with experiment. Comparable agreement was found for the present normalized one-dimensional spectra, which define a curve lying within the scatter of the Stewart & Townsend data. We can, however, extend our comparison to the three-dimensional spectra and energy transfer spectra computed by Kraichnan. To facilitate comparison we adopt Kraichnan's asymptotic scaling wave-number k_d and velocity v_d, which are related to the Kolmogoroff similarity variables by

$$k_K = (R_\lambda/\sqrt{15})^{\frac{1}{2}} k_d, \quad v_K = (R_\lambda/\sqrt{15})^{-\frac{1}{4}} v_d.$$

We shall compare our data with Kraichnan's runs number 4 and 10, for which he presented results for $T(k,t)$. Kraichnan indicated that the longest computation times used in his calculations probably corresponded to the initial period of decay in grid turbulence. We find indeed that the measurements and calculations are in closer agreement as the total elapsed computation time increases, and so we present comparisons only for the longest times used in the calculations. A difficulty in comparing Kraichnan's results with experiment is, as he noted, the dependence of the results on the essentially arbitrary choice of initial spectrum. Compared with the present measured three-dimensional energy spectra, Kraichnan's initial spectra have maxima at substantially higher wave-numbers, and the over-all shapes of the spectra are quite different. This is reflected in the comparison of the measured and computed dissipation spectra for the largest

computation times, shown in figure 14. The measured spectra are generally smaller, and exhibit a maximum at a lower wave-number. The same differences are evident in comparisons of one-dimensional spectra. The comparison of the

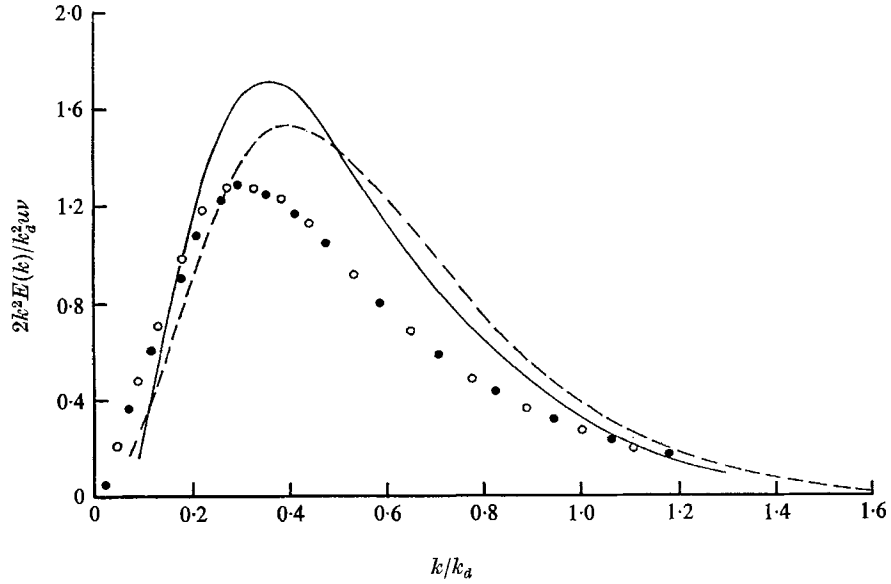

FIGURE 14. Comparison of measured dissipation spectrum with results of numerical calculations of Kraichnan. ●, U = 15·7 m/s; ○, U = 7·7 m/s. Kraichnan: ——, run 4; ----, run 10.

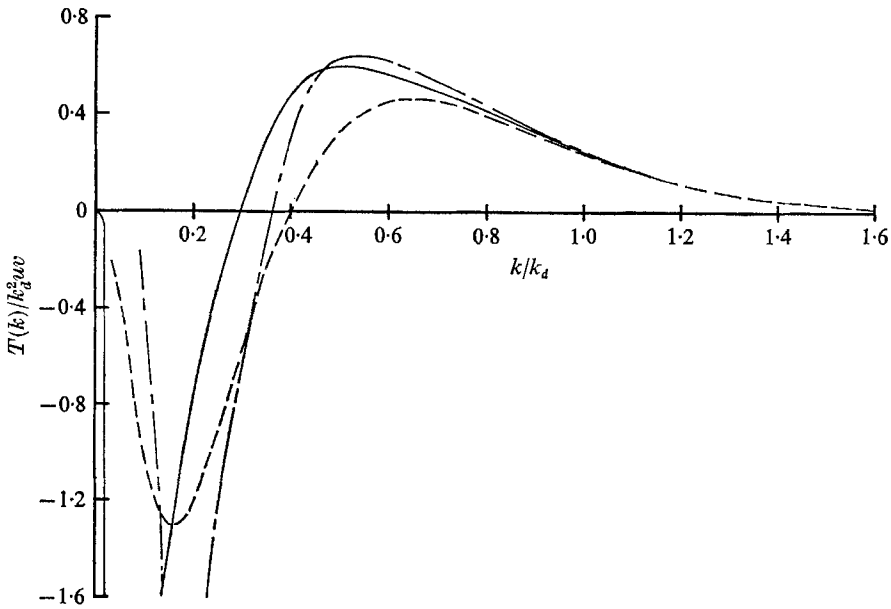

FIGURE 15. Comparison of measured energy transfer spectrum with numerical calculations of Kraichnan. ——, present measurements, x/M = 48, $R_\lambda \simeq$ 40. – – –, Kraichnan run 4, t = 1·51$L(0)/u(0)$, R_λ = 17·4; ----, Kraichnan run 10, t = 1·62$L(0)/u(0)$, R_λ = 17·7.

computed and measured energy transfer spectra in figure 15, however, shows encouraging agreement. For run 4, the measurements and calculations are in good agreement for $k/k_d \geqslant 0{\cdot}5$, and all the spectra have the same general shape throughout the high wave-number range. Furthermore, the calculated points of maximum dissipation and zero net energy transfer occur at nearly the same normalized wave-number, as was also found experimentally. The fact that this value of k/k_d is shifted to higher wave-numbers in the calculations may be a consequence of the choice of initial spectra whose maxima were also shifted toward higher wave-number. The present comparison suggests that the use of more carefully tailored, experimentally realizable, initial spectra in future calculations is certainly desirable and may provide further useful comparisons.

7. Comparison with hypotheses

Various investigators have proposed hypotheses relating $T(k)$ with $E(k)$. None of the hypotheses to date has a demonstrably sound physical basis. Most of the hypotheses have received considerable critical discussion and physical interpretation in the literature (e.g. see the discussion and bibliography of Pao 1965). Although they invariably lead to energy spectra containing an inertial subrange, most of the proposed transfer spectra themselves apply only to higher wave-numbers, as they do not behave correctly in the inertial sub-range. To be physically correct in the inertial subrange, a hypothesis for $T(E)$ should produce $T(k) \equiv 0$ over the entire inertial subrange, where $E(k) \sim k^{-\frac{5}{3}}$. When one substitutes only $E(k) = ak^{-\frac{5}{3}}$ in the various expressions for $T(E)$, the result, $T \equiv 0$, is obtained in every case, but when one includes the complete spectrum (including either the high wave-number or low wave-number region, or both) those hypotheses involving integrals of functions of E produce $T \equiv 0$ at most at a single value of k, and not over the entire inertial subrange. The physically unrealistic influence of large wave-numbers on the dynamics of the inertial subrange is a particularly degrading feature of the latter group, which includes the hypotheses of Obukhov (1941), Heisenberg (1948) and the modified versions of the hypotheses of Obukhov and Kovasznay discussed by Hinze (1959). The hypothesis of Pao (1965) and the unmodified hypothesis of Kovasznay (1943), which are differential forms that express $T(k)$ in terms of spectrally local values of $E(k)$ and dE/dk, are the only candidates that reduce to $T \equiv 0$ over the inertial subrange.

We compare the measured $T(k)$ with the transfer spectra calculated from the measured $E(k)$ using the various hypotheses. The hypotheses of Heisenberg, Kovasznay and Obukhov are of the form $T = 2Kf(E)$, where K is an undetermined constant. Figure 16 shows the comparison with Heisenberg's hypothesis and the modified Kovasznay and Obukhov hypotheses. For the latter two cases, no values for K can be found that will produce a good fit to the data, but Heisenberg's expression fits the data for large wave-numbers fairly well, using $K = 0{\cdot}25$. Uberoi found similar agreement with Heisenberg's hypothesis, with $K = 0{\cdot}2$. There is, of course, no point in fitting the low wave-number region of the data. As shown in figure 17, Kovasznay's original hypothesis cannot be scaled to fit the data, but the expression given by Pao fits the high wave-number data fairly

well. Pao's expression contains no unknown constants, other than the Kolmogoroff constant α. However, his expression fits the $T(k)$ data best if we choose $\alpha = 3{\cdot}5$, roughly twice as large as the average of the measured values of α quoted by Pao. Realizing the futility of attempting to draw meaningful physical

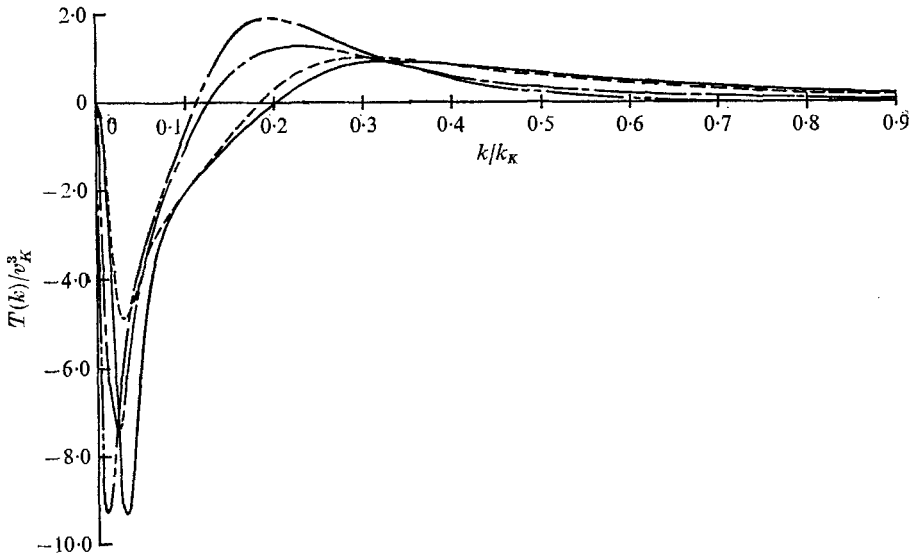

FIGURE 16. Comparison of measured transfer spectra with $T(k)$ computed from measured $E(k)$ using Heisenberg's hypothesis and modified hypotheses of Kovasznay and Obukhov. ——, Directly measured; ----, Heisenberg; $K = 0{\cdot}25$; – – – –, modified Kovasznay; — · —, modified Obukhov.

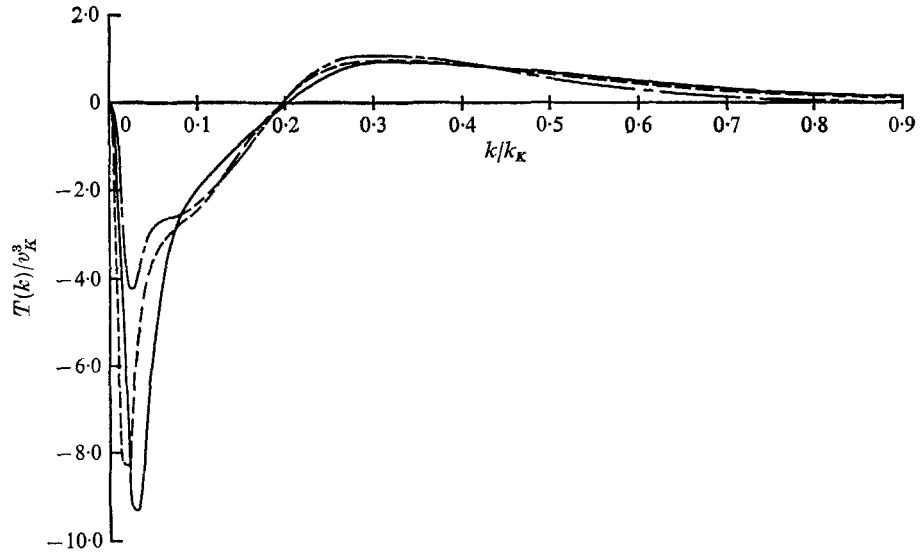

FIGURE 17. Comparison of measured transfer spectra with $T(k)$ computed from measured $E(k)$ using hypotheses of Kovasznay and Pao. ——, measured; – – –, Kovasznay; ----, Pao, $\alpha = 3{\cdot}5$.

conclusions from the various hypotheses, one hopes that more direct calculations (such as those of Kraichnan), involving no arbitrary constants, will soon become available.

8. Conclusions

The energy transfer spectrum in locally isotropic turbulence can be accurately determined from measurements of a particular combination of third-order correlation functions. For large enough wave-numbers the spectral transfer of turbulent energy in grid turbulence is adequately described (within experimental uncertainty) by the spectral energy balance equation for isotropic turbulence. The isotropic relation is accurate over roughly the same wave-number range found to be locally isotropic by considering energy spectra alone. For large wave-numbers the present measured transfer spectra may closely approximate the universal similarity range energy transfer spectrum.

The present experimental results are generally consistent with those obtained by Uberoi. However, certain operations on the data employed by Uberoi for purposes of interpretation have been found to be unnecessary or unwarranted when the complete energy balance is measured.

The degree of quantitative agreement of the measured energy transfer spectra with the results of Kraichnan's calculations for decaying isotropic turbulence encourages further calculations of this type, using initial spectra of the form observed in the laboratory.

The work was supported principally by the National Science Foundation, grant GK-1515, and partly by the Advanced Research Projects Agency (Project DEFENDER), contract no. DA-31-124-ARO-D-257, monitored by the U.S. Army Research Office, Durham.

REFERENCES

BATCHELOR, G. K. 1953 *The Theory of Homogeneous Turbulence.* Cambridge University Press.

FRENKIEL, F. N. & KLEBANOFF, P. S. 1967 *Phys. Fluids* **10**, 1737.

HEISENBERG, W. 1948 *Z. Phys.* **124**, 628.

HINZE, J. O. 1959 *Turbulence.* McGraw-Hill.

OBUKHOV, A. M. 1941 *C. R. Acad. Sci. U.S.S.R.* **32**, 19.

KOVASZNAY, L. S. G. 1948 *J. Aero. Sci.* **15**, 745.

KRAICHNAN, R. 1964 *Phys. Fluids* **7**, 1030.

PAO, Y. H. 1965 *Phys. Fluids* **8**, 1063.

STEWART, R. W. & TOWNSEND, A. A. 1951 *Phil. Trans.* A **243**, 359.

UBEROI, M. S. 1963 *Phys. Fluids* **6**, 1048.

VAN ATTA, C. W. & CHEN, W. Y. 1968 *J. Fluid Mech.* **34**, 497.

VAN ATTA, C. W. & CHEN, W. Y. 1969 *Phys. Fluids, Proc. International Symposium on High Speed Computing in Fluid Dynamics* (in the Press).